Morphology and Mechanical Properties of High-Impact Polystyrene/Elastomer/Magnesium Hydroxide Composites

Suqin Chang,[1,2] Tingxiu Xie,[3] Guisheng Yang[1,3]

[1]*CAS Key Laboratory of Engineering Plastics, Joint Laboratory of Polymer Science and Materials, Institute of Chemistry, Chinese Academy of Sciences, Beijing 100080, People's Republic of China*
[2]*Graduate School of the Chinese Academy of Sciences, Beijing 100039, People's Republic of China*
[3]*R&D Center, Shanghai Genius Advanced Materials, Shanghai 201109, People's Republic of China*

Received 23 December 2005; accepted 21 April 2006
DOI 10.1002/app.24720
Published online in Wiley InterScience (www.interscience.wiley.com).

ABSTRACT: Ternary composites of high-impact polystyrene (HIPS), elastomer, and magnesium hydroxide filler encapsulated by polystyrene were prepared to study the relationships between their structure and mechanical properties. Two kinds of morphology were formed. Separation of elastomer and filler was found when a nonpolar poly[styrene-*b*-(ethylene-*co*-butylene)-*b*-styrene] triblock copolymer (SEBS) was incorporated. Encapsulation of filler by elastomer was achieved by using the corresponding maleinated SEBS (SEBS-*g*-MA). The mechanical properties of ternary composites were strongly dependent on microstructure. In this study, the composites with separate dispersion structure showed higher elongation, modulus and impact strength than those of encapsulation structure. Impact-fracture surface observation showed that the toughening mechanism was mainly due to the massive cavitation and extensive matrix yielding. © 2006 Wiley Periodicals, Inc. J Appl Polym Sci 102: 5184–5190, 2006

Key words: high-impact polystyrene; ternary composite; mechanical properties; encapsulated magnesium hydroxide

INTRODUCTION

High-impact polystyrene (HIPS) is widely used in packaging, toys, bottles, housewares, electronic appliances, and light-duty industrial components because of its good rigidity and ease of coloring and processing. However, its poor flame resistance hinders its practical applications in some fields. Magnesium hydroxide ($Mg(OH)_2$) is a good flame retardant for its high decomposition temperature and smoke suppressibility, and widely used in thermoplastics, such as polypropylene, polyethylene, ethylene vinyl acetate, and polyamide.[1–8] However, the disadvantage of $Mg(OH)_2$ is the high level contents (more than 60%w/w) required to achieve the desired flame retardant effect. Additions of fillers in such high amounts adversely affect mechanical properties of the plastics, including reducing elongation at break, sacrificing impact strength, and increasing melt viscosity. Therefore, it is a common practice to toughen polymer/filler hybrid composites by incorporating elastomer microparticles, e.g., by physical blending of HIPS, $Mg(OH)_2$ with elastomer.

Correspondence to: G. Yang (ygs@geniuscn.com).
Contract grant sponsor: 973 Program; contract grant number: 2003CB6156002.

In the past few decades, there have been many reports of investigations related to thermoplastics/elastomer/filler systems,[9–21] most of which have focused on polyolefin materials. But, the possible presence of matrix–filler, matrix–rubber, and rubber–filler interfaces in the ternary composites results in a complexity of phase structure[22] and a corresponding variation of the composite properties.

On the other hand, in a highly filled polymer system, a major problem is nonuniformity of properties due to poor dispersion of the filler in the matrix.[23] The traditional method of treating filler surface by low-molecular coupling agents or surfactants has been found to be reasonably effective due to reducing interfacial tension between fillers and polymer matrix. However, such low-molecular agents with very short chains, e.g., stearic acid, are hard to anchor to the polymer matrix through physical entanglements and van der Waals interactions.[24,25] Recently, another new method called ''*in situ* polymerization'' has been proposed.[26–28] *In situ* polymerization is a method in which inorganic particles are first dispersed into suitable monomers, and this mixture is then polymerized using a technique similar to bulk polymerization. Magnesium hydroxide used in this work was coated with PS by *in situ* encapsulation method developed in our laboratory. It was expected that the PS covered on the surface of $Mg(OH)_2$ could improve dispersion of the particles

in matrix and enhance the interfacial adhesion between filler–elastomer and/or filler–matrix, leading to improve mechanical properties and processability of the resulting composites. Further studies on the surface treatment procedures of $Mg(OH)_2$ and the characterization of PS coated $Mg(OH)_2$ will be summarized in another study.

The main purpose of this article was to investigate influences of thermoplastic elastomers on the interfacial properties, morphology, and mechanical properties, e.g., stiffness, strength, and toughness of magnesium hydroxide filled HIPS. Two kinds of thermoplastic elastomers were used: poly[styrene-*b*-(ethylene)-*b*-styrene] triblock copolymer (SEBS) and the corresponding block copolymer grafted with maleic anhydride (SEBS-*g*-MA).

EXPERIMENTAL

Materials

HIPS (PH-88HT, melt flow index = 4.5 g/10 min at 200°C and 5 kg) with density 1.04 g/cm^3 was provided by Zhenjiang Chimei. Magnesium hydroxide, employed as filler, was a high purity untreated grade (Magnifin H5) supplied by Martinswerk. The volume average particle size was 1.5 μm, and the specific surface area was 5.0 m^2/g. Magnesium hydroxide was coated with PS by *in situ* encapsulation method developed in our laboratory before compounding. Poly [styrene-*b*-(ethylene-*co*-butylene) (SEBS) triblock copolymer, Kraton^{TM} G1652 was supplied by Shell Chemicals (29% styrene, molecular weights: styrene block7000, EB block 37,500). Poly[styrene-*b*-(ethylene-*co*-butylene)-*b*-styrene] (SEBS-*g*-MA) triblock copolymer, Kraton^{TM} FG1901X was supplied by Shell Chemicals (29% styrene, nominal weight of grafted maleic anhydride = 1.8 ± 0.4%, quoted at 1.84% as measured by elemental analysis[29]).

Surface treatment of magnesium hydroxide

Magnesium hydroxide ($Mg(OH)_2$) powder was dried at 120°C for 6 h, and then was put into high speed mixer by heated to 70°C with a rotation speed of 1200 rpm. Then, acetone solutions of 3-(methacryloxy) propyltrimethoxy silane (MPS) with water and acetic acid was added under stirring for 20 min. The modified powder was dried at 80°C for 12 h. Finally, modified powder, monomer (styrene), and additional initiator (AIBN) were placed into the mixer with agitation fixed at 1200 rpm and heated in an oil bath at 80°C for 45 min.

Preparation of composites

HIPS was first mixed with PS-coated $Mg(OH)_2$ and SEBS(or SEBS-*g*-MA) in a high-speed mixer for 20 min. Then, the mixture was extruded in a corotating twin screw extruder with an L/D ratio of 42 and screw diameter of 35 mm. The temperature profiles of the barrel were 180, 190, 200, 210, 210, and 215°C from the hopper to the die, respectively, and the screw speed was 400 rpm. A series of composites with different composition were obtained as shown in Table I. The specimens for mechanical tests were molded with an injection molding machine and the injection temperature was 210°C.

Characterization of structure and properties

The cryogenic fractured surfaces of specimens were etched with hydrochloric acid for 2 h to remove the uncoated magnesium hydroxide particles, and then were gold-sputtered. The surfaces of specimen images were observed on scanning electron microscope (SEM) (JSM-6360LV, JEOL, Japan) with an accelerating voltage of 10 kV.

The tensile testing was performed on a universal testing machine (SANS, Shenzhen, China), according to ASTM D638 with a cross-head speed of 50 mm/min. The Izod notched impact strength was measured with an impact testing machine (XJU-22, Chengde, China), according to ASTM D256. All experiments were conducted at room temperature and a relative humidity (RH) of 50%.

RESULTS AND DISCUSSION

Morphology of ternary composites

The morphology of binary composites of HIPS/$Mg(OH)_2$ and HIPS/coated $Mg(OH)_2$ is presented for comparative purpose. In Figures 1(a–b), both of the composites had been etched by hydrochloric acid. The voids shown in the picture were vacancies left by the removal of $Mg(OH)_2$ particles dispersed in the HIPS matrix. It can be clearly seen from

TABLE I
Weight and Volume Percentages in Ternary HIPS Composites

HIPS/elastomer/coated $Mg(OH)_2$			
HIPS/SEBS/coated $Mg(OH)_2$		HIPS/SEBS-*g*-MA/coated $Mg(OH)_2$	
wt %	vol %	wt %	vol %
100/0/0	100/0/0	80/20/0	78.0/22.0/0
80/20/0	78.0/22.0/0	60/20/20	66.0/24.7/9.3
60/20/20	66.0/24.7/9.3	50/20/20	58.7/26.3/15
50/20/20	58.7/26.3/15	40/20/40	50.3/28.2/21.5
40/20/40	50.3/28.2/21.5	30/20/50	40.7/30.4/28.9
30/20/50	40.7/30.4/28.9	20/20/60	29.5/33.0/37.5
20/20/60	29.5/33.0/37.5		

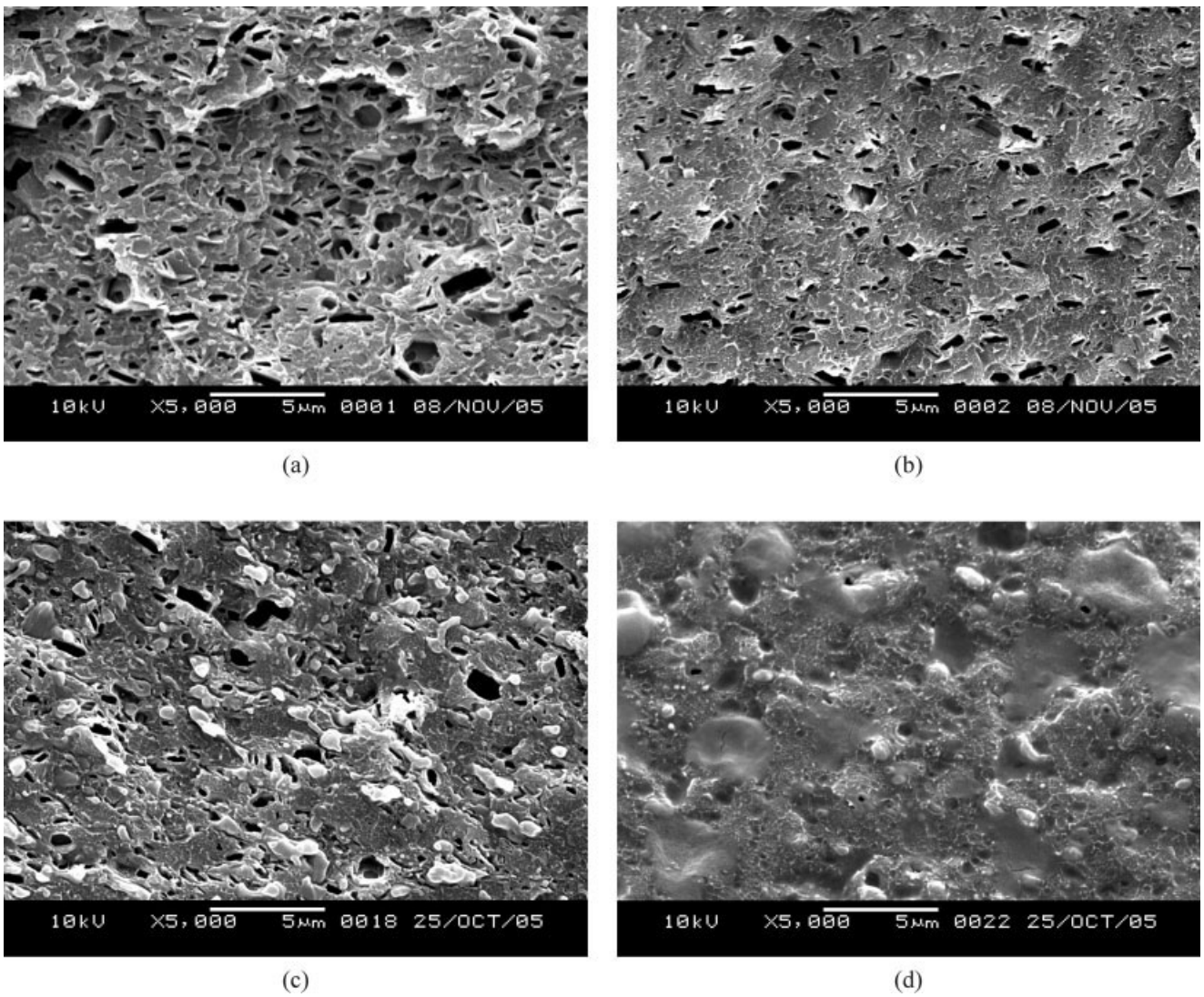

Figure 1 Scanning electron micrographs of etched surface of ternary phase HIPS composites. (a) HIPS/uncoated $Mg(OH)_2$ (60/40); (b) HIPS/coated $Mg(OH)_2$ (60/40); (c) HIPS/SEBS/coated $Mg(OH)_2$(40/20/40); (d) HIPS/SEBS-*g*-MA/coated $Mg(OH)_2$(40/20/40).

Figure 1(a) that the uncoated $Mg(OH)_2$ particles in the binary composites of HIPS/$Mg(OH)_2$ were completely etched with hydrochloric acid due to the very poor interfacial adhesion. The broad size distribution of dispersion phase indicated that there existed seriously particle agglomeration. However, for the coated $Mg(OH)_2$ based composites, the etched holes appeared to be evenly distributed in the matrix without obvious particle agglomeration, as shown in Figure 1(b). In addition, much less voids appeared compared with uncoated $Mg(OH)_2$ based composites, confirming that the $Mg(OH)_2$ particles were partially encapsulated with PS during the *in situ* treatment with styrene monomers. This result demonstrated that incorporation of the PS chemically bonded on the $Mg(OH)_2$ surface could prominently improve the dispersion of filler particles in the matrix and enhance the interfacial adhesion between them.

In ternary composites of polymer/elastomer/inorganic filler, the dispersion state of elastomer and filler plays an important role in determination of properties of composites. To investigate their morphologies, the cryogenic fractured surfaces of samples were also etched by hydrochloric acid.

Scanning electron micrographs of the etched cryogenic fracture surfaces of HIPS/SEBS/$Mg(OH)_2$ and HIPS/SEBS-*g*-MA/$Mg(OH)_2$ composites are shown in Figures 1(c–d). The dark holes represented the etched $Mg(OH)_2$ particles. The number of dark holes of HIPS/SEBS/$Mg(OH)_2$ system shown in Figure 1(c) was almost the same when compared with that of coated $Mg(OH)_2$ based composites [Fig. 1(b)]. This suggested that the $Mg(OH)_2$ particles were evenly

TABLE II
Tensile Properties of Ternary HIPS Composites

HIPS/Elastomer/ $Mg(OH)_2$ (vol %)	Tensile strength (MPa)		Elongation at break (%)	
	SEBS	SEBS-*g*-MA	SEBS	SEBS-*g*-MA
100/0/0		32.5		42
78.0/22.0/0	23.7	23	61	85
66.0/24.7/9.3	22	19.5	34	23
58.7/26.3/15	20.2	19.1	35	14
50.3/28.2/21.5	18.2	18.3	28	13
40.7/30.4/28.9	16.9	16.9	20	11
29.5/33.0/37.5	14.6	15.3	20	11

TABLE IV
Impact Properties of Ternary HIPS Composites

HIPS/Elastomer/ $Mg(OH)_2$ (vol %)	Impact strength (KJ/m^2)	
	SEBS	SEBS-*g*-MA
100/0/0		24
78.0/22.0/0	41	35
66.0/24.7/9.3	18	7.5
58.7/26.3/15	20	5.8
50.3/28.2/21.5	17	5.0
40.7/30.4/28.9	14	3.8
29.5/33.0/37.5	13	3.5

distributed in the matrix, while there was no evidence of SEBS encapsulation around the filler, resulting in a separate dispersion of SEBS and $Mg(OH)_2$ particles in the HIPS matrix.

For the HIPS/SEBS-*g*-MA/$Mg(OH)_2$ system, a contrasting morphology is shown in Figure 1(d). Voids were not observed. This result demonstrated that the introduction of SEBS-*g*-MA could further encapsulate the $Mg(OH)_2$ particles due to the strong interaction between maleic anhydride groups of SEBS-*g*-MA and the $Mg(OH)_2$ particles unencapsulated by PS. The complete encapsulation of $Mg(OH)_2$ particles prevented them being etched by hydrochloric acid. Thus, the core–shell structure in SEBS-*g*-MA based ternary composites was obtained.

Mechanical properties

The influences of the concentration of SEBS, SEBS-*g*-MA, and $Mg(OH)_2$ on composite tensile properties are shown in Table II. Incorporation of elastomer to HIPS led to a reduction in tensile strength of both binary blends of HIPS/SEBS and HIPS/SEBS-*g*-MA. At the same volume fraction of the filler, the tensile strength of both systems was almost the same. These results indicated that the polarity of elastomer had little influence on tensile strength of both ternary composites. But the ternary system containing SEBS had higher elongation than that of the composites containing SEBS-*g*-MA.

TABLE III
Flexural Properties of Ternary HIPS Composites

HIPS/Elastomer/ $Mg(OH)_2$ (vol%)	Flexural strength (MPa)		Flexural modulus (GPa)	
	SEBS	SEBS-*g*-MA	SEBS	SEBS-*g*-MA
100/0/0		50.7		2.2
78.0/22.0/0	36.8	36.1	1.4	1.4
66.0/24.7/9.3	35.8	32.8	1.8	1.2
58.7/26.3/15	33.3	31.9	1.7	1.1
50.3/28.2/21.5	30.9	30.4	1.8	1.0
40.7/30.4/28.9	32.2	28.3	2.2	1.0
29.5/33.0/37.5	25.9	26.0	2.0	1.0

The flexural properties of ternary composites of HIPS/SEBS/$Mg(OH)_2$ and HIPS/SEBS-*g*-MA/$Mg(OH)_2$ are shown in Table III. It was evident that incorporation of 22 vol % elastomer markedly reduced the modulus of HIPS in both binary HIPS/SEBS and HIPS/SEBS-*g*-MA blends, whereas the addition of filler could noticeably increase the modulus of the ternary HIPS/SEBS/$Mg(OH)_2$ composites. However, the modulus of ternary composites containing SEBS-*g*-MA decreased with increasing filler content. When the content of $Mg(OH)_2$ was up to 21.5 vol % and more, it had no influence on the modulus of the system. This indicated that the reinforcing efficiency of filler in the HIPS/SEBS-*g*-MA/$Mg(OH)_2$ composites was suppressed by the encapsulation structure of $Mg(OH)_2$ with SEBS-*g*-MA. The lowering in modulus of composites with an encapsulation structure have been reportedly due to the volume of low modulus elastomer inclusion extended by the rigid filler core, thus leading to a decrease in composite modulus.[30] As shown in Table III, the elastomer type was little influence on the flexural strength of ternary composites.

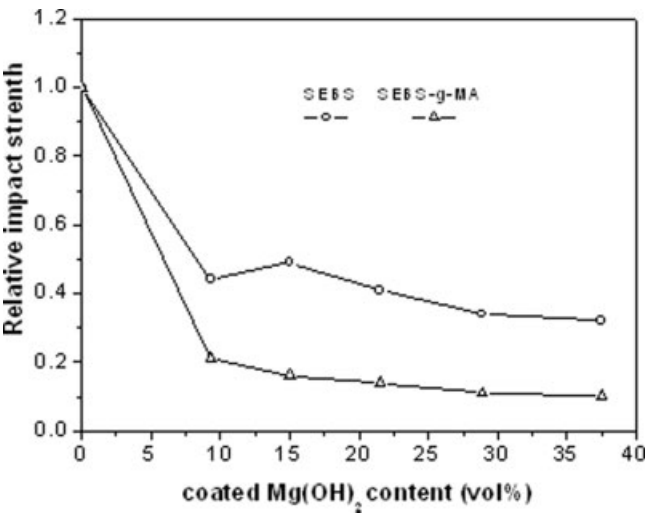

Figure 2 Effect of filler content on the relative impact energy of HIPS composites (○) composites containing SEBS; (□) composites containing SEBS-*g*-MA.

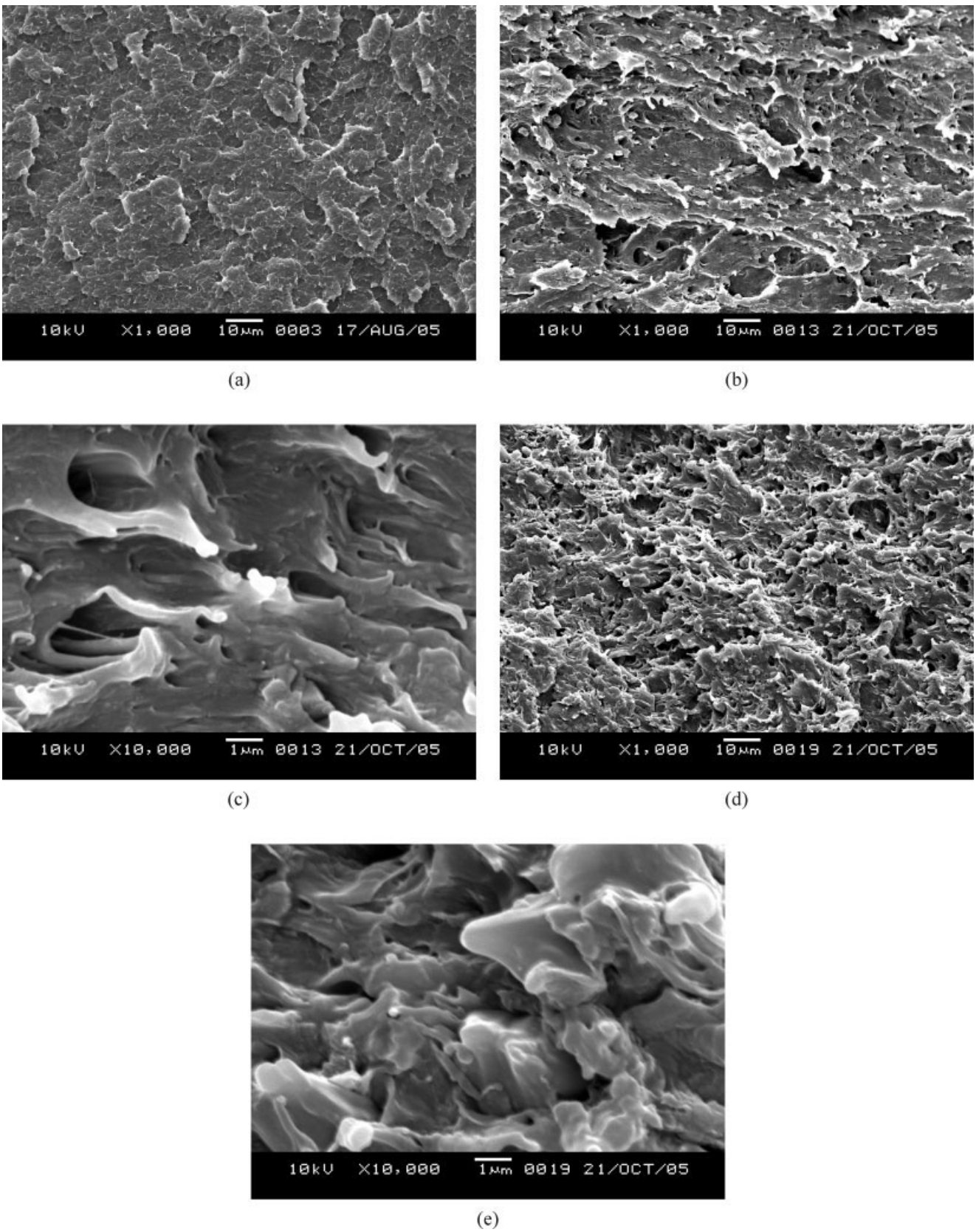

Figure 3 Impact fractured surfaces of HIPS and HIPS/elastomer blends. (a) pure HIPS; (b) HIPS/SEBS (80/20) at low magnification; (c) high magnification of (b); (d) HIPS/SEBS-*g*-MA (80/20) at low magnification; (e) high magnification of (d).

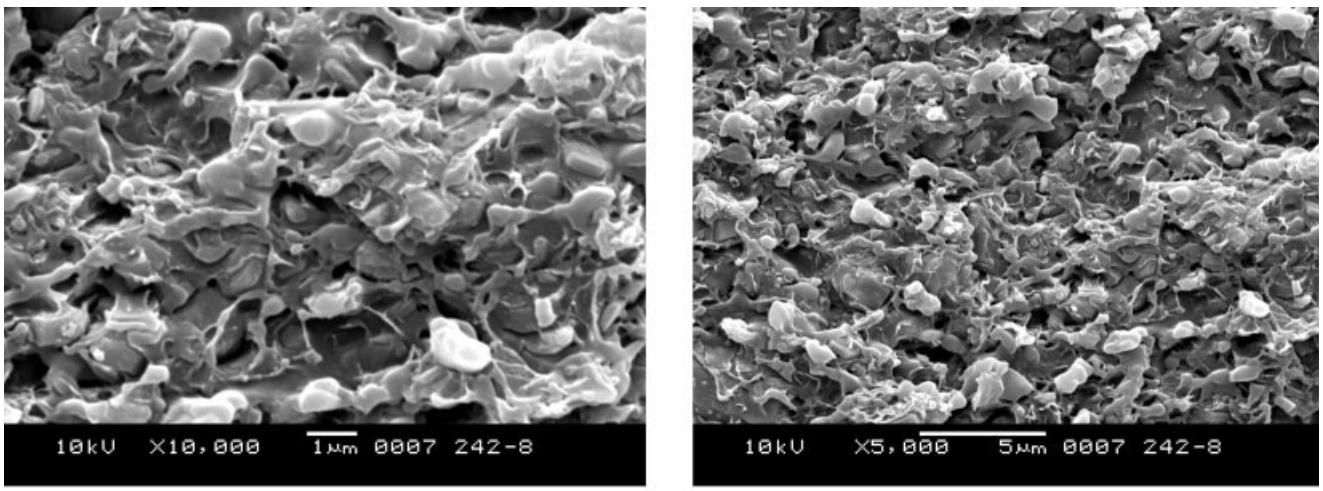

Figure 4 Impact fractured surfaces of HIPS and HIPS/SEBS/coated $Mg(OH)_2$ (40/20/40) composites (a) at low magnification; (b) high magnification of (a).

Table IV shows the notched Izod impact strength of various HIPS composites. In binary blends, the impact strength of HIPS was significantly increased with incorporation of elastomers, in particular SEBS. In the ternary system, SEBS was far more effective in improvement of composite impact resistance than HIPS. The difference in impact strength of both systems might be caused partly by elastomer itself. To eliminate the effect of elastomer characteristics, the relative impact strength was considered. Plots of the relative impact strength as a function of filler concentration are presented in Figure 2. In the case of HIPS/SEBS/$Mg(OH)_2$ composites, a sharp decrease of the impact energy occurred at 9.3 vol % filler loadings. Further increase of filler concentration beyond 15 vol % caused only a little drop in impact energy. In the HIPS/SEBS-*g*-MA/$Mg(OH)_2$ composites, although an encapsulation structure of filler by elastomer was achieved, a drop in composite impact strength was much more pronounced. These results showed that the separated dispersion of elastomer and filler in the matrix was much more effective to maintain the impact strength than the complete encapsulation of fillers at the same concentration.

Fractography

Investigations of the deformation mechanism were performed with SEM analysis of their impact-fracture surfaces of HIPS/elastomer/$Mg(OH)_2$ composites. Figure 3(a) shows scanning electron micrographs of impact-fracture surface of pure HIPS.

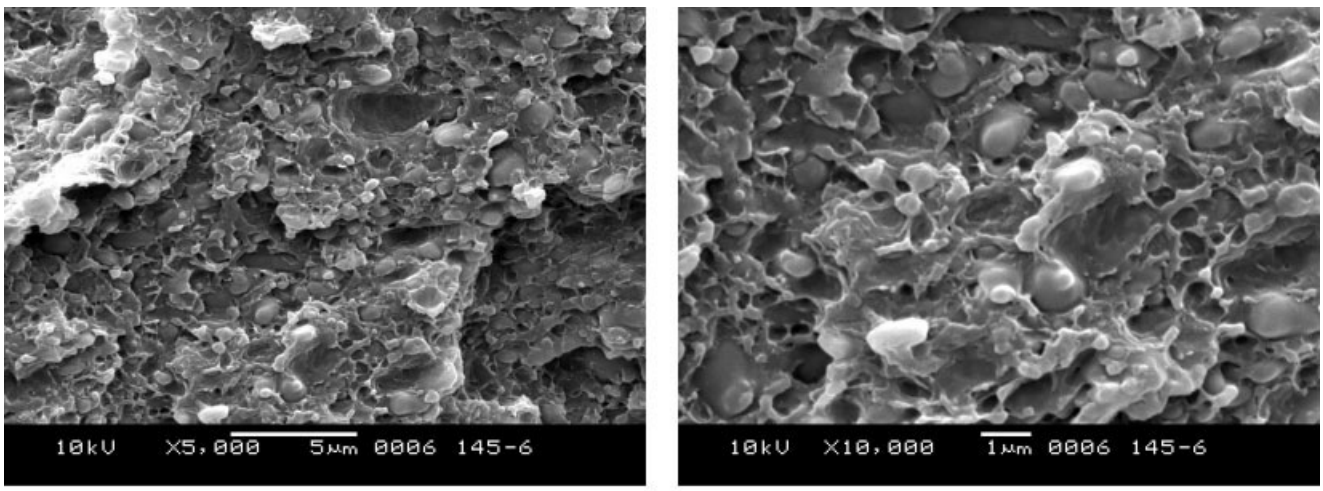

Figure 5 Impact fractured surfaces of HIPS and HIPS/SEBS-*g*-MA/coated $Mg(OH)_2$ (40/20/40) composites. (a) At low magnification; (b) high magnification of (a).

It was evident that HIPS exhibited brittle fracture style. Incorporation of SEBS to HIPS led to extensive plastic deformation as shown in Figure 3(b–c). Comparing with the HIPS/SEBS binary blends, the fracture surface observed in the HIPS/SEBS-*g*-MA system [Fig. 3(d–e)] showed much less plastic deformation.

In the HIPS/SEBS/coated $Mg(OH)_2$ composites, as shown in Figure 4(a,b), fibril-like structure was formed at the interface, surrounding the filler particles debonding from the matrix. Moreover, the matrix ligaments exhibited considerable plastic deformability. Such fibril-like structures were also found in the binary HIPS/SEBS [Figs. 4(a–b)] and have been reported in other rubber modified polymers.[31–33] This result suggested the introduction of SEBS could improve the deformability of the polymer matrix, leading to a considerable increase in the impact strength of the SEBS based composites.

However, the debonding degree of $Mg(OH)_2$ particles dramatically decreased in the SEBS-*g*-MA based composites. As shown in Figure 5(a–b), many filler particles immersed in the SEBS-*g*-MA, instead of debonding from the matrix during the deformation process. This might be attributed to the strong interaction between the filler and matrix. The filler particle debonding was dominated by debonding stress, which depended on the interfacial adhesion between the filler and matrix.[34] The improvement in the interfacial adhesion by SEBS-*g*-MA led to an increase in the debonding stress, which restricted the filler particle debonding process. On the other hand, the incorporation of elastomer resulted in a dramatic decrease in the tensile yield stress. Once the debonding stress was higher than the tensile yield stress, the yielding of the matrix took place, rather than the debonding of filler particles.[35] Thus, the debonding process was hindered, leading to much lower impact strength than that of HIPS/SEBS/coated $Mg(OH)_2$ system.

CONCLUSIONS

The effects of elastomer type on morphology and mechanical properties of ternary HIPS composites containing elastomer and $Mg(OH)_2$ coated by polystyrene were investigated. Morphology, as obtained by SEM, revealed a separated dispersion of elastomer and filler particles for SEBS-based ternary composites, and a complete encapsulated structure for SEBS-*g*-MA based ones was observed.

The differences of the mechanical properties between two kinds of ternary composites were marked. Composites with separately dispersed particles of elastomer and filler had higher elongation, modulus and impact strength than composites with core–shell particles. Analysis of impact fracture morphology revealed that extensive plastic deformation of the matrix and cavitation resulted from filler–matrix debonding were main toughening mechanisms for such composites.

References

1. Titelman, G. I.; Gonen, Y.; Keidar, Y.; Bron, S. Polym Degrad Stab 2002, 77, 345.
2. Hippi, U.; Mattila, J.; Korhonen, M.; Seppälä, J. Polymer 2003, 44, 1193.
3. Sain, M.; Park, S. H.; Suhara, F.; Law, S. Polym Degrad Stab 2004, 83, 363.
4. Shehata, A. B. Polym Degrad Stab 2004, 85, 577.
5. Clerc, L.; Ferry, L.; Leroy, E.; Marie, J.; Lopez-Cuesta, J. M. Polym Degrad Stab 2005, 88, 504.
6. Li, Z. Z.; Qu, B. J. Polym Degrad Stab 2003, 81, 401.
7. Rothon, R. N.; Hornsby, P. R. Polym Degrad Stab 1996, 54, 383.
8. Hornsby, P. R.; Watson, C. L. J Mater Sci 1995, 30, 5347.
9. Premphet, K.; Horanont, P. Polymer 2000, 41, 9283.
10. Ou, Y. C.; Guo, Q. T.; Fang, X. P.; Yu, Z. Z. J Appl Polym Sci 1999, 74, 2397.
11. Barteczak, Z.; Argon, A. S.; Cohen, R. E.; Weinberg, M. Polymer 1999, 40, 2347.
12. Wang, Y.; Lu, J.; Wang, G. H. J Appl Polym Sci 1996, 64, 1275.
13. Premphet, K.; Horanont, P. J Appl Polym Sci 1999, 74, 3445.
14. Jancar, J.; Dibenedetto, A. T. J Mater Sci 1994, 29, 4651.
15. Premphet, K.; Preechachon, I. J Appl Polym Sci 2003, 89, 3557.
16. Zhang, L.; Li, C. Z.; Huang, R. J Polym Sci Part B: Polym Phys 2004, 42, 1656.
17. Premphet, K.; Horanont, P. J Appl Polym Sci 1998, 70, 587.
18. Kolarik, J.; Jancar, J. Polymer 1992, 33, 4961.
19. Zhang, L.; Li, C. Z.; Huang, R. J Polym Sci, Part B: Polym Phys 2005, 43, 1113.
20. Pukanszky, B.; Tudos, F.; Kolarik, J.; Lednicky, F. Polym Compos 1990, 11, 98.
21. Kolarik, J.; Pukanszky, B.; Lednicky, F. In Interfaces in Polymer, Ceramic, and Metal Matrix Composites; Ishida, H., Ed.; Elsevier: New York, 1998; p 453.
22. Pukanszky, B.; Tudos, F.; Kularik, J.; Lednicky, F. Polym Commun 1990, 31, 201.
23. Toensmeier, P. A. Mod Plastics Int 1988, 18, 29.
24. Jancor, J.; Kucera, J Polym Eng Sci 1990, 30, 714.
25. Rahma, F.; Fellahi, S. Polym Compos 2000, 21, 175.
26. Ou, Y. C.; Yang, F.; Chen, J. J Appl Polym Sci 1997, 64, 2317.
27. Ou, Y. C.; Yang, F.; Yu, Z. Z. J Polym Sci, Part B: Polym Phys 1998, 36, 789.
28. Xie, X. L.; Li, B. G.; Pan, Z. R. J Mater Sci Eng 1999, 17, 63.
29. González, M. A.; Keskkula, H.; Paul, D. R. Polymer 1995, 36, 4587.
30. Long, Y.; Shanks, R. A. J Appl Polym Sci 1996, 62, 639.
31. Premphet, K.; Preechachon, I. J Appl Polym Sci 2000, 76, 1929.
32. Muratoglu, O. K.; Argon, A. S.; Cohen, R. E.; Weinberg, M. Polymer 1995, 36, 921.
33. Barteczak, Z.; Argon, A. S.; Cohen, R. E.; Weinberg, M. Polymer 1999, 40, 2331.
34. Pukanszky, B.; Voros, G. Compos Interfaces 1993, 1, 411.
35. Yin, J.; Zhang, Y.; Zhang, Y. X. J Appl Polym Sci 2005, 98, 957.